

Structural diradical character

B. Alexander Voigt,¹ Torben Steenbock,² and Carmen Herrmann^{1, a)}

¹⁾*Institute for Inorganic and Applied Chemistry, Martin-Luther-King-Platz 6, University of Hamburg, 20146 Hamburg, Germany*

²⁾*Institute of Physical Chemistry, Grindelallee 117, University of Hamburg, 20146 Hamburg, Germany*

(Dated: 30 August 2018)

A reliable first-principles description of singlet diradical character is essential for predicting nonlinear optical and magnetic properties of molecules. Since diradical and closed-shell electronic structures differ in their distribution of single, double, triple and aromatic bonds, modeling electronic diradical character requires accurate bond-length patterns, in addition to accurate absolute bond lengths. We therefore introduce structural diradical character, which we suggest as an additional measure for comparing first-principles calculations with experimental data. We employ this measure to identify suitable exchange–correlation functionals for predicting the bond length patterns and electronic diradical character of a biscobaltocene with the potential for photoswitchable nonlinear optical activity. Out of four popular approximate exchange–correlation functionals with different exact-exchange admixtures (BP86, TPSS, B3LYP, TPSSh), the two hybrid functionals TPSSh and B3LYP perform best for diradical bond length patterns, with TPSSh being best for the organometallic validation systems and B3LYP for the organic ones. Still, none of the functionals is suitable for correctly describing relative bond lengths across the range of molecules studied, so that none can be recommended for predictive studies of (potential) diradicals without reservation.

^{a)}Electronic mail: Carmen.Herrmann@chemie.uni-hamburg.de

I. INTRODUCTION

Open-shell singlet diradical molecules have aroused interest among both theoreticians and experimentalists due to their special physical and chemical properties.^{1–10} Among those are their nonlinear optical (NLO) properties, especially the second hyperpolarizability, which can be tuned and amplified by a change in open-shell diradical character y ^{11–17}. Nonlinear optically active molecular materials are important for applications such as data storage and telecommunication¹⁸.

It would be particularly useful if the NLO properties of molecules or molecular materials could be switched by external stimuli. There has been considerable experimental^{19–23} and theoretical^{20,24–27} work on switchable organic and organometallic NLO-active molecules, showing that a variety of stimuli such as pH, temperature, redox reactions, and light can be used for this purpose.

The singlet state of diradicals can have a bond length pattern more reminiscent of an open-shell structure (Figure 1, top right), of a closed-shell structure (Figure 1, top left), or somewhere in between. A perfect open-shell molecular structure will typically be very close to that of a triplet. Depending on which side the molecular structure leans to, electronic properties will be considerably different, in particular the (electronic) diradical character. Indeed, it has been shown that diradical character and NLO properties can be very sensitive to molecular structure^{28–31}. Open-shell electronic structures have also been found to depend on interatomic distances in the context of strongly correlated adsorbates and materials^{32–34}. For predicting diradical properties from first principles, it is therefore important to predict sufficiently accurate molecular structures, both in terms of absolute bond lengths and in terms of bond length patterns.

For many diradicals of interest, Kohn–Sham (KS)-density functional theory (DFT) is the only first-principles electronic structure method capable in practice of molecular structure predictions with reasonable accuracy (see also Appendix C). Yet, owing to the unknown exchange–correlation functional, DFT can give inconclusive results regarding such structures.

We are interested in a particular example of such inconclusive predictions, a dithienylethene-linked biscobaltocene whose diradical properties could be switched, in principle, by light (see Figure 2). In combination with the redox-active nature of the cobaltocene units, this might

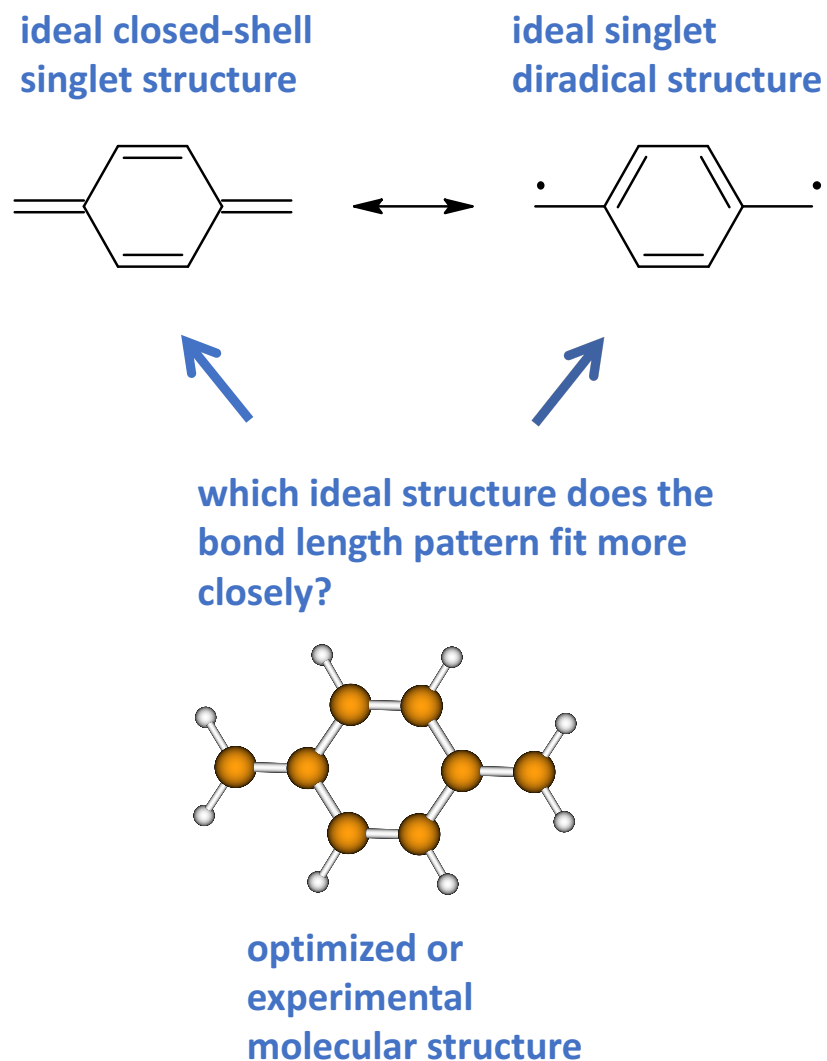


FIG. 1. Our measure of structural diradical character is based on comparing bond-length patterns of molecular structures with idealized bond-length patterns for closed- (top left) and open-shell diradical (top right) forms, shown here for p-quinodimethane.

lead to multiresponse behavior. Closing the photoswitch (left-hand side of Figure 2) switches on electronic communication via the π system of the bridge, which enables drawing two different structures, a closed-shell one (Figure 3, left) and an open-shell one (Figure 3, right). The relative importance of these two not only affects NLO properties, but a stabilization of the closed switch resulting from a large admixture of the closed-shell form can also suppress photochromic ring opening^{35,36}. Due to its poor switching behavior, the closed-switch form could not be isolated experimentally, and its structure and properties are therefore not known yet³⁷. To decide whether further efforts towards obtaining these data and towards

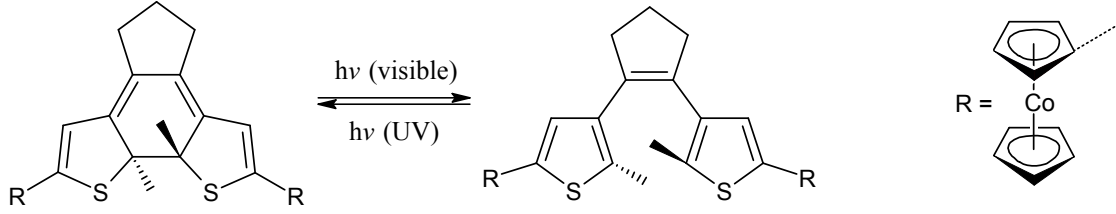


FIG. 2. Lewis structures of a dithienylethene molecule in its closed (left) and open form (right).

optimizing the switching behavior are worthwhile, we aim at a true first-principles prediction of the diradical character of the closed switch. In contrast to the analogous nitronyl nitroxide compound³⁸ (see Supplemental Material), KS-DFT optimizations of the molecular structure for the closed switch in its singlet state give no consistent answer to whether it is predominantly a closed-shell or an open-shell structure (see Section IV). Consequently, no predictions of its diradical character and its NLO properties appear possible, unless a particular approximate exchange–correlation functional can be identified as sufficiently reliable for this purpose.

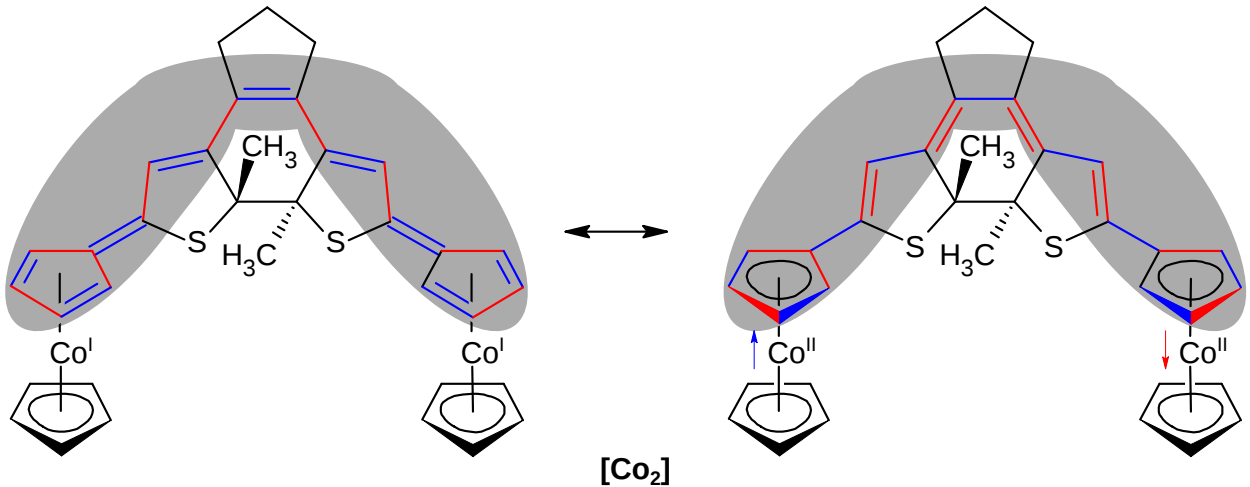


FIG. 3. Lewis structures of $[\text{Co}_2]$. The closed-shell quinoidal form is shown on the left-hand side, the diradicaloid form on the right-hand side. Note that strictly speaking, these are not mesomeric forms, since bond lengths will differ between the diradicaloid and the closed-shell structures. The bonds whose formal bond orders and thus lengths differ between the two structures are indicated by the grey area. Bonds included in evaluating established BLA measures are shown in red if they were added and in blue if they were subtracted in Eq. (A1)^{39,40}.

One would expect that bond-length alternation (BLA)^{39,40} was a good measure for com-

paring molecular structures optimized with different approximate exchange–correlation functionals and experimental structures. It turns out that BLA values spread so unsystematically that this is not possible (along with other disadvantages, as discussed in Appendix A). Therefore, we will define a new measure for this purpose, which we call structural diradical character (see Section II A). It is based on measuring the deviation of bond lengths for a structure of interest from ideal bond lengths of (a) an open-shell singlet and (b) a closed-shell singlet (see Figure 1), obtained with the same methodology as the structure of interest (DFT with a particular exchange–correlation functional, or experiment). We will show below that this indeed allows for identifying functionals that can be considered reliable for bond length patterns of singlet diradicals. For this purpose we will analyze a series of experimentally studied diradicals (see Figures 4 and 5).

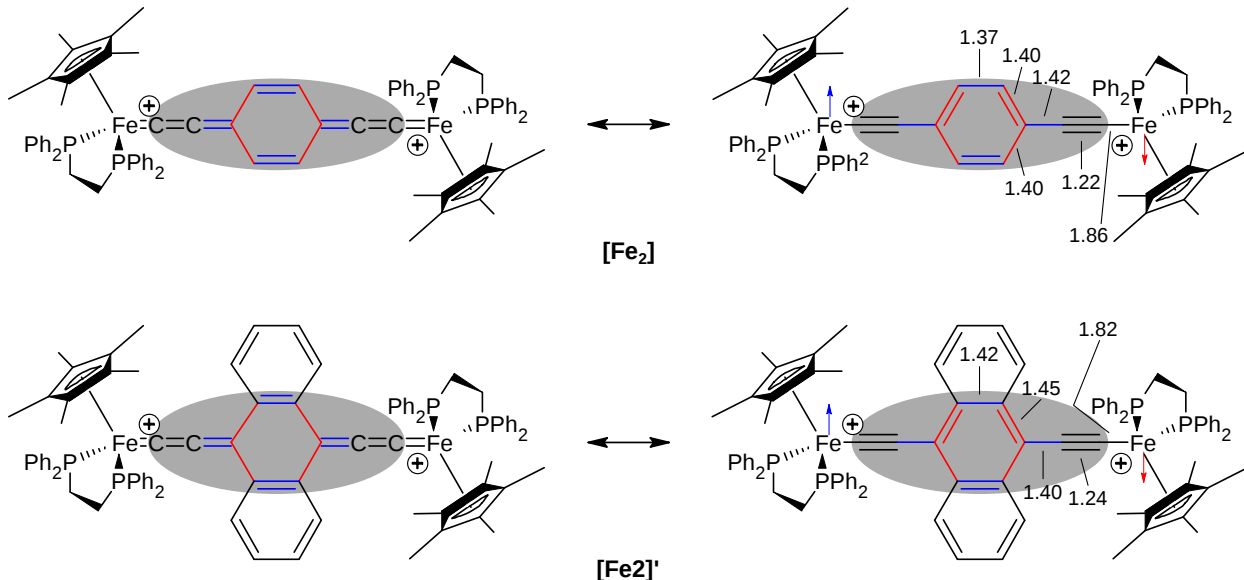


FIG. 4. Lewis structures of $[\text{Fe}_2]$ and $[\text{Fe}_2]'$. The bond lengths (in Å) for $[\text{Fe}_2]$ and $[\text{Fe}_2]'$ are taken from X-ray crystal structures from Ref.⁴¹ and⁴², respectively. Note that the shown structures are, strictly speaking, not resonance structures, since they have different bond lengths. Bonds included in evaluating established BLA measures are shown in red if they were added and in blue if they were subtracted in Eq. (A1)^{39,40}. Note that the reference bond lengths within the benzene rings were those of aromatic benzene and not the alternating single and double bonds shown in the Lewis structures. Also, the Fe–C bonds are not included in the evaluation of the structural diradical character, because no reference bond length for Fe–C single and Fe=C double bonds were defined.

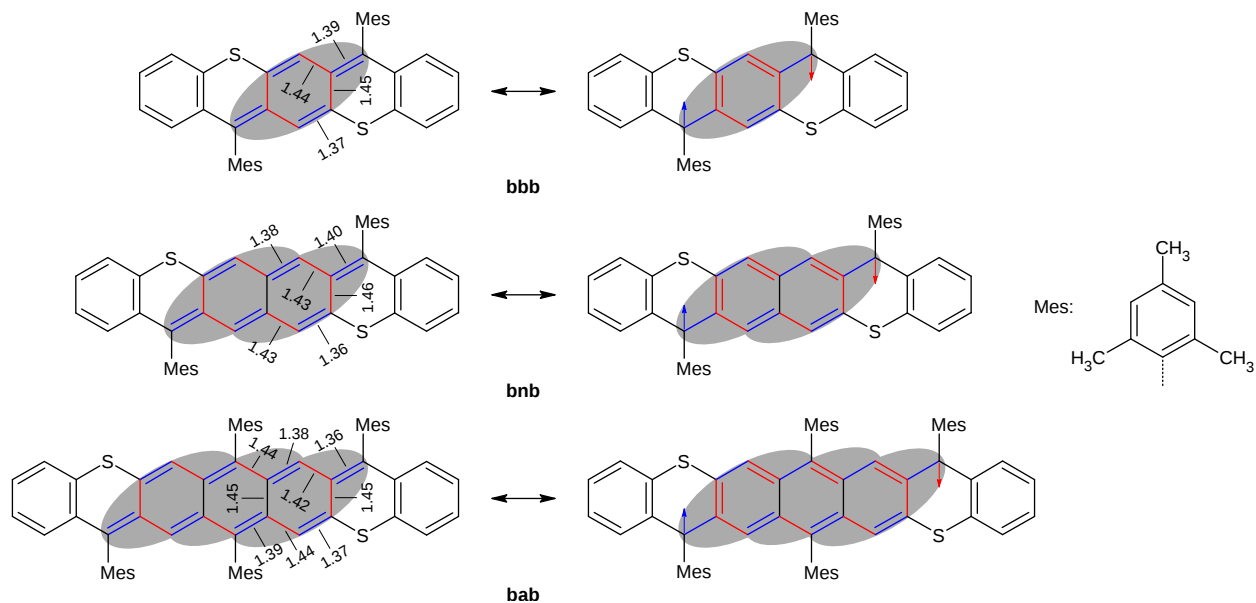


FIG. 5. Lewis structures and selected X-ray crystallographic bond lengths (from Ref.⁴³) of **bbb**, **bnb** and **bab**. The closed-shell quinoidal form is shown on the left-hand side, the diradicaloid form on the right-hand side. Note that strictly speaking, these are not mesomeric forms, since bond lengths will differ between the diradicaloid and the closed-shell structures. Bonds included in evaluating established BLA measures are shown in red if they were added and in blue if they were subtracted in Eq. (A1)^{39,40}.

II. STRUCTURAL DIRADICAL CHARACTER

Diradical character is a measure used to indicate how close a system resembles one with two unpaired electrons (usually in a singlet state). Open-shell character is a more general term that can be used in various contexts. It may refer to diradical character (two unpaired electrons) as well as to any other polyradical character (any number of unpaired electrons). Here, we use the terms diradical character and open-shell character synonymously.

A. Defining structural diradical character: How close is the bond length pattern of a molecular structure to that an ideal diradical?

We introduce a new measure for estimating the qualitative similarity of a molecular structure to an ideal diradical or closed-shell bond pattern (see Figure 1). The new measure overcomes the drawbacks of the BLA scheme while still retaining its simplicity. For this

purpose, reference bond lengths for the ideal open-shell and closed-shell structures have to be defined (see Section IIB below for details). The actual bond lengths b for the structure of interest are then compared to these reference bond lengths b_{ref} , and the normalized mean absolute error ($\text{MAE}_{\text{norm}}^X$; $X = \text{CS}, \text{OS}$),

$$\text{MAE}_{\text{norm}}^X = \frac{\sum_{i=1}^n \frac{|b_i - b_{i,\text{ref}}^X|}{|b_{i,\text{ref}}^{\text{OS}} - b_{i,\text{ref}}^{\text{CS}}|}}{n}, \quad (1)$$

and the normalized root mean squared deviation ($\text{RMSD}_{\text{norm}}^X$; $X = \text{CS}, \text{OS}$),

$$\text{RMSD}_{\text{norm}}^X = \sqrt{\frac{\sum_{i=1}^n \left(\frac{b_i - b_{i,\text{ref}}^X}{|b_{i,\text{ref}}^{\text{OS}} - b_{i,\text{ref}}^{\text{CS}}|} \right)^2}{n}}, \quad (2)$$

are calculated for all n bonds where the reference bond length in the closed-shell state (CS) and open-shell state (OS) differ (these bonds are encapsulated in gray ovals in the corresponding Figures). The normalization is used to account for different magnitudes in reference bond-length differences (20 pm for a C–C \longrightarrow C=C transition, 14 pm for a C=C \longrightarrow C \equiv C transition, 14 pm for a C–C \longrightarrow C=C transition and 6 pm for a C=C \longrightarrow C=C transition).

The structural diradical character y_s is then defined as

$$y_s = 1 - \frac{\text{MAE}_{\text{norm}}^{\text{OS}}}{\text{MAE}_{\text{norm}}^{\text{OS}} + \text{MAE}_{\text{norm}}^{\text{CS}}} = \frac{\text{MAE}_{\text{norm}}^{\text{CS}}}{\text{MAE}_{\text{norm}}^{\text{OS}} + \text{MAE}_{\text{norm}}^{\text{CS}}}. \quad (3)$$

The structural diradical character can be calculated from the $\text{RMSD}_{\text{norm}}^X$ in an analogous way.

B. Choosing reference bond lengths for diradical and closed-shell structures

It is not quite obvious how ideal diradical and closed-shell singlet bond lengths should be defined. One option would be to carry out a computational structure optimization in which the electronic structure is constrained to be a closed-shell singlet (as in spin-restricted KS-DFT) and to use the resulting bond lengths as references for the closed-shell structure, and, accordingly, a spin-unrestricted triplet optimization for a “perfect” open-shell structure. This has the obvious disadvantage that it cannot be applied to experimental structures.

Another option is to interpret the Lewis structures literally and to use C–C bond lengths of ethane, ethene, ethine, and benzene, . . . as references. These ideal bond lengths are obtained with the same method as the molecular structure of interest, i.e., either by structure optimization with a method like DFT (see Supplemental Material for values), or from tabulated experimental data for these validation compounds (taken from Ref⁴⁴)⁴⁵. The drawback of this definition is that a “real-world” open-shell singlet may be quite far from a perfect bond pattern as shown on the left-hand side of Figure 1, because π conjugation⁴⁶, chemical substitution, intramolecular and intermolecular dispersion interactions and repulsions, and other effects may lead to deviations from ideal bond lengths. For the same reasons, what we would clearly consider a closed-shell singlet structure may deviate from its ideal bond pattern as shown on the right-hand side of Figure 1. We do not consider this a major problem, because these reasons are present in computationally optimized and experimental structures alike. We do acknowledge that (1) in practice, intermolecular interactions are usually neglected in DFT (but this is the case for nearly all computational work) and (2) in cases where a certain exchange–correlation functional has a weakness concerning, e.g., intramolecular dispersion interactions indirectly affecting bond length patterns, we may not be able to disentangle intrinsic problems of this functional with bond length patterns from its weaknesses with dispersion. However, with these exceptions, we consider comparing the structural diradical character between experiment and computation as a valuable means of gaining insight into the reliability of electronic structure methods for molecular structure optimizations of diradicals.

III. AN ILLUSTRATIVE EXAMPLE: ELECTRONIC DIRADICAL CHARACTER DEPENDS ON BOND LENGTH PATTERNS MUCH MORE THAN ON ABSOLUTE BOND LENGTHS

The studied molecules can be drawn in different forms (see Figures 3, 4 and 5), one of which denotes a CS and the other an OS form bearing two unpaired electrons. These two forms differ in the distribution of C–C bonds (single-, double-, triple- and aromatic bonds) between respective carbon atoms. In the CS, the bond lengths are typically more equally distributed than in the OS. These bond length distributions or bond length patterns can be used to evaluate the structural diradical character.

We will show in the following that the structural diradical character correlates more with electronic diradical character^{28,47–52} than the MAE of absolute bond lengths does. To illustrate this (see Figure 6), we have compared the correlation of structural diradical character and MAE of a set of different structures of p-quinodimethane.

First, we describe the construction of the studied set of structures. We take two structures as end points for a linear interpolation: First, a structure resembling the closed-shell Lewis structure was built and its bond lengths were chosen to be the ideal bond lengths that are used as a reference in the calculation of the structural diradical character (see Table S3 in the Supporting Information). This structure then has a structural diradical character of 0. We will call this structure ideal closed shell or cs-id. The second structure was constructed in a similar fashion, but this time, the ideal bond lengths resembling the open-shell Lewis structure were chosen, resulting in a structural diradical character of 1. Analogously, this structure is referred to as ideal open shell or os-id. The 11 studied structures (see Section S8 in the Supporting Information for cartesian coordinates) were then built as linear interpolations between cs-id (with weights between 0.0 and 0.2, the latter being referenced as cs-20 = 0.2·cs-id + 0.8·os-id) and os-id (with weights between 1.0 and 0.8). The weights were chosen to be in a region where the electronic diradical character is sensitive to structural changes. We computed the electronic diradical character y_{el} , structural diradical character y_s , and the MAE of the bond lengths that were used for calculating y_s (the C–C bond lengths) with respect to a fictitious “validation” structure which is a linear combination of os-id (weight is 0.9) and cs-id (weight is 0.1), denoted as ref. The latter structure corresponds to what would usually be a molecular structure from the experiment, and was chosen such that it is in the middle of the range of structural mixtures under study.

The better correlation between electronic and structural diradical character than between electronic diradical character and the MAE is evident. The Pearson correlation coefficient between y_s and y_{el} (Figure 6, left) is 1.00, while it is 0.07 between MAE and y_{el} (Figure 6, right). For the realistic systems under study, we will show that structural diradical character shows a similarly better correlation with electronic diradical character than MAE (see Figures 7 and 8).

Accordingly, correct bond length patterns are more important for getting electronic diradical character right than only good agreement with absolute bond lengths. In particular, good agreement with absolute bond lengths may lead to considerable deviations in electronic

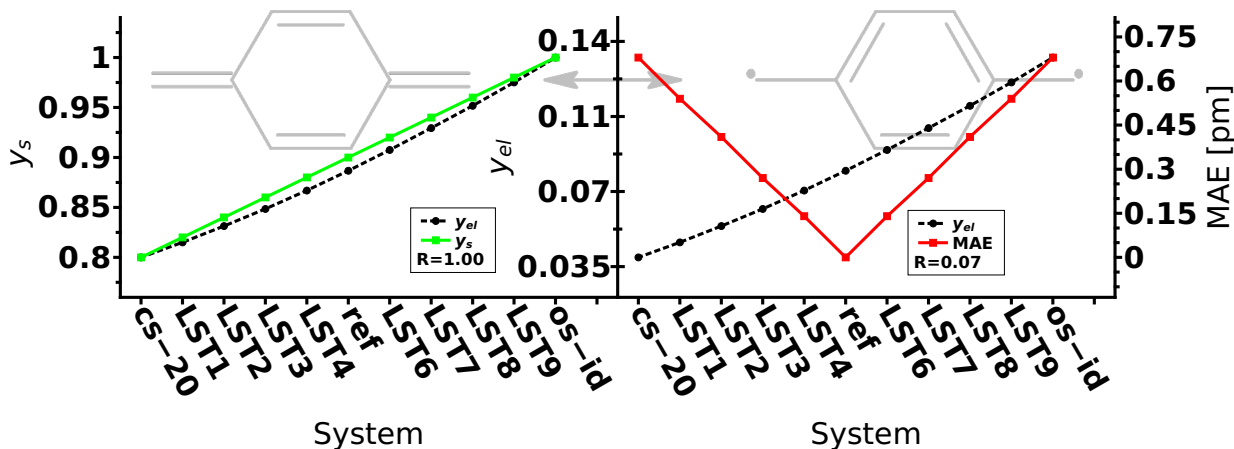


FIG. 6. Comparison of the correlation between electronic (y_{el}) and structural (y_s) diradical character (MAE, Equation (3)) on the left (right). The Pearson correlation coefficient R is shown in the corresponding legends. The systems are p-quinodimethanes with different bond lengths. cs-20 (ref, os-id) is a linear combination of 20 % (10 %, 0 %) cs-id and 80 % (90 %, 100 %) os-id, the structures denoted as LST*i* are linear combinations of $20 - 2i$ % cs-id and $80 + 2i$ % os-id. To make a qualitative comparison easier, the scales of the ordinates were chosen so as to have the smallest (and largest) data points of the respective curves on equal heights. Single point calculations used B3LYP/def2-TZVP-D3.

diradical character if it was obtained at the expense of realistic bond length patterns. We therefore suggest a measure for the agreement with bond length patterns as an important additional criterion when evaluating the performance of electronic structure methods for molecular structure optimizations of diradicals, in addition to measures for absolute bond length deviations.

IV. ATTEMPT AT A TRUE FIRST-PRINCIPLES PREDICTION OF DIRADICAL CHARACTER: BISCOBALTOCENYLDITHIENYLETHENE

Dithienylethene (DTE) derivatives can, in principle, be switched from a closed form (Figure 2 left), which has an extended conjugation, to an open form (Figure 2 right) by radiation with visible light. Ring closure can be initiated by irradiation with UV light (due to a less extended conjugation in the open form). For the closed form with the attached cobaltocenes ($[\text{Co}_2]$), a diradical Lewis structure with two unpaired electrons and a closed-

shell structure with no unpaired electrons can be drawn (see Figure 3). It is not known yet experimentally whether the molecule is predominantly OS or CS in its ground state.

In an attempt to make a true first-principles prediction on this question, we have calculated optimized structures (open and closed shell) and analyzed the spin-state energetics and structural diradical characters of this compound, employing the pure BP86 functional and the hybrid B3LYP with 20 % admixture of Hartree–Fock exchange. We start molecular structure optimizations for (1) a closed-shell singlet (cs), employing spin-restricted KS DFT (RKS), (2) a broken-symmetry⁵³ (bs) approximation of the open-shell singlet employing spin-unrestricted KS DFT (UKS), for which the local spin density in the initial guess corresponded to one spin-up unpaired electron on one spin center and one spin-down electron on the other center⁵⁴, and (3) a triplet (t) described by UKS to evaluate singlet–triplet splittings. For a bs solution with approximately one unpaired electron per spin center, a total spin expectation value of $\langle \hat{S}^2 \rangle$ close to one is expected⁵⁵. The bs approach may converge to a closed-shell solution, which is indicated by $\langle \hat{S}^2 \rangle$ approaching zero. Therefore, $\langle \hat{S}^2 \rangle$ values are reported for all cs and bs optimizations. All molecular structures under study have singlet ground states.

TABLE I. Relative energies with respect to the closed-shell energy (ΔE) [kJ/mol], structural diradical character y_s (Equation 3) (MAE and, in parentheses, RMSD), bond-length alternation (Equation A1) BLA [pm], \hat{S}^2 expectation values ($\langle \hat{S}^2 \rangle$) for the optimized structures of [**Co**₂] (see Figure 3) employing BP86/def2-TZVP and B3LYP/def2-TZVP, for closed-shell (cs), open-shell singlet modeled by a broken-symmetry (bs) determinant, and triplet (t). The structural diradical characters of the energetically most stable structures are highlighted in green (with energies differing by less than 5 kJ/mol considered as degenerate). The overall assignment as closed-shell (CS) or open-shell (OS) is indicated in the right-most column.

	cs				bs				t			
	ΔE	y_s	BLA	$\langle \hat{S}^2 \rangle$	ΔE	y_s	BLA	$\langle \hat{S}^2 \rangle$	ΔE	y_s	BLA	
	BP86											
[Co ₂]	0.00	0.58 (0.71)	2.6	0.00	1.37	0.58 (0.71)	2.6	0.01	28.45	0.67 (0.81)	-1.43	CS
	B3LYP											
[Co ₂]	0.00	0.56 (0.67)	4.4	0.00	-52.6	0.73 (0.87)	-3.4	1.10	2.04	0.74 (0.88)	-3.7	OS

For all optimized structures, we evaluate structural diradical character and BLA. If these data agreed reasonably well for the ground-state structures of both BP86 and B3LYP, a DFT prediction of the open-shell character of $[\text{Co}_2]$ could be considered as reliable. However, BP86 gives a closed-shell structure, while B3LYP results in an open-shell singlet as the energetically most stable solution (Table I).

The structural diradical character is small for the closed-shell solutions and large for the open-shell solution, which could only be converged with B3LYP, not with BP86, even if performing a single-point calculation on the open-shell optimized B3LYP structure with the open-shell B3LYP orbitals as initial guess. Interestingly, the BP86 closed-shell singlet shows a larger structural diradical character than the B3LYP one, indicating that even though both are equally closed-shell in terms of electronic structure ($\langle \hat{S}^2 \rangle = 0$), the BP86 molecular structure leans more towards the open-shell side. For comparison, structural diradical character was also evaluated for the triplet. Here, one would expect bond length patterns close to the open-shell resonance structures, and accordingly, y_s is always largest for the triplet. For the B3LYP open-shell singlet, y_s is nearly identical to the value for the triplet, which could be taken as an additional indication that the open-shell-singlet B3LYP solution converges to a nearly pure diradical.

Here, MAE- and RMSD-derived structural diradical characters deviate by up to 0.14, with the latter being larger, while in our validation systems (see below), it does not matter much whether structural diradical character y_s is evaluated with MAE or RMSD as a measure for structural deviations, and the latter is typically slightly smaller. This different behavior might be related to the fact that single / double bond alternation plays a more pronounced role here in *both* structures in contrast to the validation compounds. This does not affect the suitability of y_s for comparisons between calculated and experimental data. It makes employing y_s as an absolute measure for diradical character difficult, but as will be discussed below, 0.6 as evaluated based on MAE appears to be a reasonable measure for the transition from what is typically considered more closed-shell to more open-shell singlet, at least for the set of molecules considered here.

A negative BLA would be expected for an open-shell structure, because the single bonds of the bridge are subtracted (blue in Figure 3) and the double bonds (shorter) are added (red in Figure 3) and the aromatic bonds (same bond lengths in the reference) will not bias the BLA towards positive or negative values. On the other hand, a positive BLA indicates a

closed-shell structure, because then the single bonds are added (red in Figure 3), while the double bonds (shorter) are subtracted (blue in Figure 3). The BLA (Equation A1) obtained from the BP86 solutions is small, but positive, rather corresponding to a closed shell, while the BLA obtained from B3LYP is positive for the closed-shell solution and negative for the open-shell solution.

In accordance with the larger open-shell character suggested by B3LYP, the singlet–triplet gap is by more than an order of magnitude smaller than the gap predicted by BP86.

Altogether, these data suggest that according to BP86, $[\text{Co}_2]$ is mostly a closed-shell molecule, while B3LYP suggests it is mostly open-shell. Therefore, in the following we will compare these two exchange–correlation (xc) functionals employed along with two meta-GGA based ones (TPSS and TPSSh) with experimental data on structures where varying the bridge modifies the diradical character.

V. COMPARISON OF DFT WITH EXPERIMENTAL MOLECULAR STRUCTURES

A. Selection of diradicals and exchange–correlation functionals

For organic diradicals, the B3LYP exchange–correlation functional (with 20 % exact exchange admixture) generally works well⁵⁶, but even here, BLA^{39,40} as present in the closed-shell form on the left-hand side of Figure 1 can be underestimated⁵⁷ or overestimated^{30,58}, depending on the molecule studied. While numerous studies on the dependence of NLO properties on exchange–correlation functional have been carried out^{29,59–73}, it is not clear if there is a reasonably reliable functional for describing bond length patterns for organometallic complexes with potential diradical character.

We therefore apply the structural diradical measure defined in Section II to two sets of selected organometallic^{41,42} and organic⁴³ validation compounds for which structural data are available from the experiment for given spin centers with two and three different bridges, respectively, and where these variations of the bridge are known to change the diradical character considerably (see Figures 4 and 5). Even though the organometallic systems are quite large molecules, we consider, in contrast to previous work^{41,42}, the full atomistic details of all ligands.

We compare four different exchange–correlation functionals, three of which (BP86, TPSS, TPSSh) have proven valuable for structures and energetics of transition metal complexes^{74–76}, while B3LYP is very popular for open-shell organic molecules. BP86 and TPSS are pure functionals, and TPSSh and B3LYP are hybrid functionals with 10 and 20 percent of exact-exchange admixture, respectively. The pure parts of BP86 and B3LYP are of generalized gradient corrected (GGA) type, and for TPSS and TPSSh, of meta GGA type. Since exact exchange admixture tends to localize spin density^{77–79}, hybrid functionals should favor diradical structures (right-hand side of Figure 1) more strongly than pure ones.

B. Inorganic validation systems: Dinuclear carbon complexes with carbon-rich bridges

In the two dicationic complexes shown in Figure 4, two iron(III) centers with one unpaired electron each are linked by carbon-rich bridges, in one case with a benzene linker ($[\mathbf{Fe}_2]$) and in one case with a benzene linker featuring two annelated rings ($[\mathbf{Fe}_2]'$). This annelation should decrease the aromaticity of the central carbon structure, and thus favor the cumulenenic structure shown on the left-hand side.

Indeed, in the experiment⁴², analysis of characteristic bond lengths (Fe–C, –C≡C, ≡C–C) of $[\mathbf{Fe}_2]$ revealed longer Fe–C and ≡C–C and shorter –C≡C bonds as compared to the X-ray structure of $[\mathbf{Fe}_2]'$, indicating a larger structural diradical character. Despite slight differences, this holds for both molecules present in the unit cell (indicated by “xray1” “and xray2” in the lower part of Table S4 in the Supporting Information)⁸⁰. Superconducting quantum interference device (SQUID) magnetometry (as powder) revealed a singlet ground state for $[\mathbf{Fe}_2]$ with a thermally accessible triplet state about 4.56 kJ/mol higher in energy, suggesting that the ground state has significant open-shell character. The variable temperature (VT)-UV-Vis spectra did not give any evidence of structural changes between 10 K and 300 K, and VT-IR spectra pointed to a barely detectable increase of cumulenenic character with decreasing temperature, suggesting that the structural changes between the singlet and triplet states are minor. Altogether, this was interpreted as $[\mathbf{Fe}_2]$ having significant open-shell singlet character in its ground state, despite the relatively strong antiferromagnetic spin coupling.

For $[\mathbf{Fe}_2]'$, no signal was found in the electron spin resonance (ESR) spectrum at 77 K,

so the triplet state is not thermally accessible up to that temperature, corresponding to a singlet–triplet splitting of at least 1200 cm^{-1} (roughly 14.3 kJ/mol). This is also supported by VT-NMR data. IR spectra support the more cumulenic structure that was also indicated by X-Ray crystallography. This points to $[\mathbf{Fe}_2]'$ having substantial closed-shell character in the ground state.

Figure 7 shows that hybrid functionals, in particular B3LYP and TPSSh, can describe the structural diradical character of $[\mathbf{Fe}_2]$ very well (compare the solid and dotted green lines). For $[\mathbf{Fe}_2]'$, B3LYP overestimates this character somewhat, while TPSSh is very close to the experimental value (please see Section S5 in the Supporting Information for tabulated data). Interestingly, the reduction in y_s from $[\mathbf{Fe}_2]$ to $[\mathbf{Fe}_2]'$ is partially described already by the closed-shell-optimized structures. For the open-shell (bs) optimized structures, y_s increases as spins become more localized on the spin centers (as indicated by increasing $\langle \hat{S}^2 \rangle$ in Table S4 in the Supporting Information). This is in line with this localization indicating a stronger importance of the open-shell resonance structure (right-hand side of Figure 4). The B3LYP open-shell-singlet structure for $[\mathbf{Fe}_2]$ has a y_s very close to the value for the triplet, which suggests that B3LYP would consider $[\mathbf{Fe}_2]$ almost purely open shell. For TPSSh, the values are also reasonably close, indicating dominant open-shell character.

Owing to the size of the systems under study (we describe all ligands in full atomistic detail), crystal structure optimizations under periodic boundary conditions (in particular with hybrid functionals) are prohibitively expensive. It has been pointed out that crystal packing can increase quinoidal character⁵⁸, so our first-principles structural diradical characters for isolated molecules may overestimate the values obtained from X-ray crystallography somewhat. At least for $[\mathbf{Fe}_2]$, measured exchange spin coupling constants were very similar in the solid state and in solution⁴², which suggests that structural differences between the two are not major. Still, it may be that the deviation of B3LYP data from the experiment is partially due to the neglect of packing effects.

Overall, based on the structural diradical character y_s , TPSSh would be considered adequate for describing the two iron-based complexes under study here (with B3LYP being also acceptable). TPSSh also matches the experimental singlet–triplet energy splitting for $[\mathbf{Fe}_2]$ quite nicely (2.9 kJ/mol vs. 4.56 kJ/mol), and is not too far from the experimental lower bound on this splitting for $[\mathbf{Fe}_2]'$ (8.1 kJ/mol vs. 14.3 kJ/mol), whereas B3LYP underestimates both.

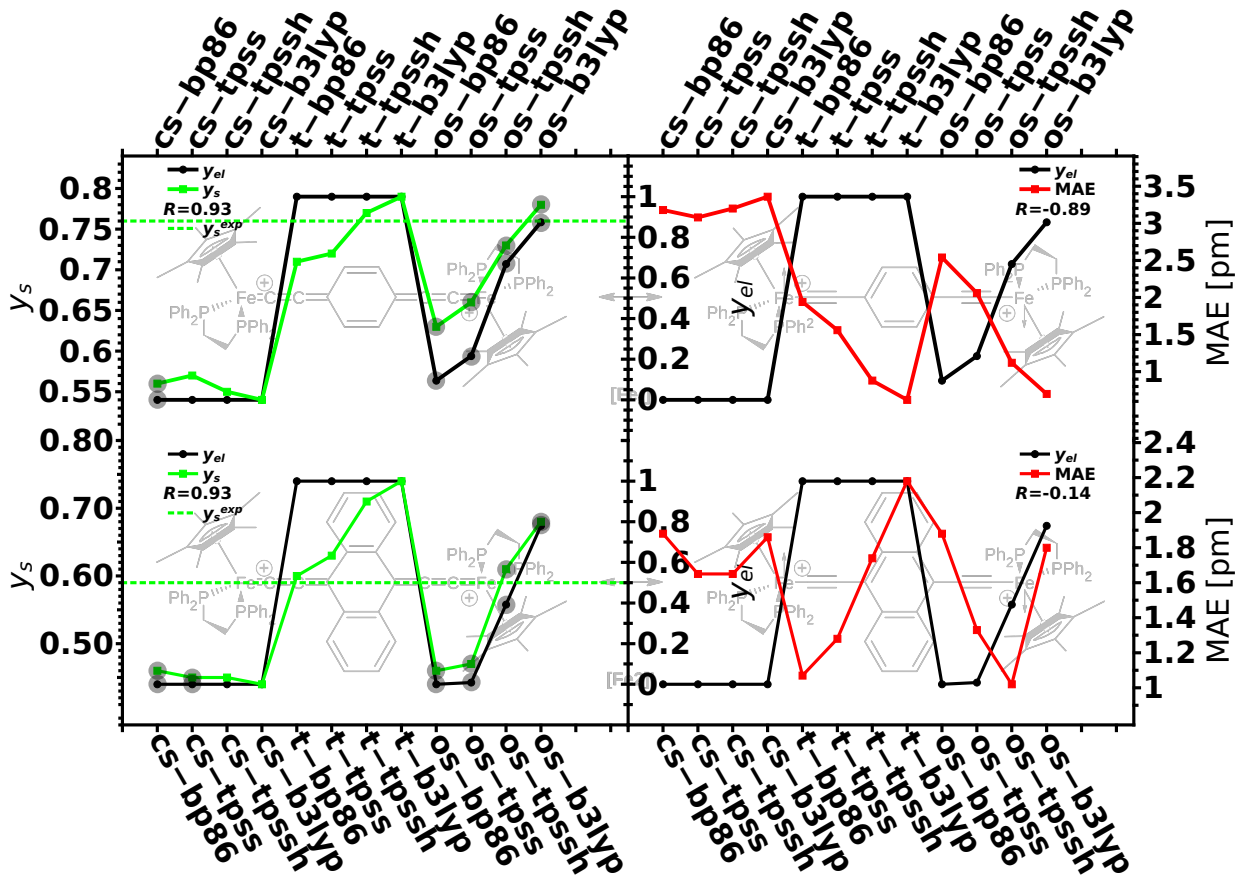


FIG. 7. Comparison of the correlation between electronic diradical character y_{el} and structural diradical character y_s (MAE) on the left (right). MAE values are calculated from geometry optimized and experimental structures. The Pearson correlation coefficient R is shown in the corresponding legends. The data for $[\text{Fe}_2]$ ($[\text{Fe}_2]'$) are shown in the top (bottom) half. Values for y_{el} , y_s and MAE are plotted against a string representing the calculated determinant (either cs for closed shell, t for triplet or os for broken symmetry) and the used xc functional. Additionally, the calculated structural diradical character values for the x-ray structures y_s^{exp} are plotted as a constant dotted line. The energetically most stable structures are highlighted by a circular grid on top of the data point. Again, energies differing by less than 5 kJ are considered degenerate, leading to multiple highlighted structures per functional in some cases.

In Section III, we showed that the structural diradical character y_s correlates with the electronic diradical character y_{el} and that only taking into account averaged absolute bond length deviations MAE does not suffice for a reliable comparison of computed and experi-

mental data. An analysis of the correlation between y_s and y_{el} and between MAE and y_{el} has been conducted for the experimental validation systems as well (see Figure 7). Again, we see that structural diradical character correlates more strongly with electronic diradical character than MAE. The correlation (expressed through the Pearson correlation coefficient R) is 0.93 between y_s and y_{el} and -0.89 between MAE and y_{el} . Here, strong anticorrelation between MAE and y_{el} is observed, because the system under study is open shell. There, one would expect the MAE between the experimental structure and the optimized one to be larger for the closed-shell structure (where y_{el} is small) and smaller for open-shell structures (where y_{el} is large). The weak correlation between MAE and electronic diradical character at $[\mathbf{Fe}_2]'$ is attributed to the higher level of complexity in the bonding patterns. While in the organic systems, only alternations between single-, double- and aromatic bonds happen, while in the inorganic systems, alternations between single-, double-, aromatic- and triple bonds take place. The structural diradical character can clearly deal with these complex bonding patterns.

With bond-length alternation, it is more difficult to obtain a clear picture (see Supporting Information Table S4). Bond-length alternation should be more pronounced for the more quinoidal form of $[\mathbf{Fe}_2]'$ compared with $[\mathbf{Fe}_2]$, and this is indeed the case for the structures obtained from experiment. Also, the BLA of an open-shell solution (if one is converged) is, as expected, smaller than for a closed-shell solution. For the DFT-optimized structures, BLA data vary significantly depending on the xc functional employed. The increase in BLA from $[\mathbf{Fe}_2]$ to $[\mathbf{Fe}_2]'$ is only reproduced for the two pure functionals (for which attempts at broken-symmetry optimizations converge to $\langle \hat{S}^2 \rangle$ smaller than one), and in terms of absolute numbers, there is no functional which agrees well with the BLA for both $[\mathbf{Fe}_2]$ and $[\mathbf{Fe}_2]'$. For $[\mathbf{Fe}_2]$, B3LYP comes closest (but fails for $[\mathbf{Fe}_2]'$), and for $[\mathbf{Fe}_2]'$, TPSS matches best (but strongly overestimates BLA for $[\mathbf{Fe}_2]$). Also, while y_s changes only slightly when varying bond lengths within the experimental error bar, these variations affect BLA values considerably. All this suggests that in contrast to y_s , it is at least difficult to identify a reliable xc functional for structural diradical character based on BLA.

C. Organic validation systems: bisbenzothiaquinodimethanes with varying bridge lengths

Bisbenzothiaquinodimethanes (see Figure 5) have recently been presented as stable analogues of larger acenes, enabling the experimental study of diradical character as a function of molecular length⁴³. While all three molecules under study showed considerable quinoidal character, diradical character increased with increasing molecular length as expected, owing to the increasing number of aromatic rings formed in the open-shell resonance structure⁸¹. This was concluded, among others, from the X-Ray crystallographic structures and from the increased spectral broadening in VT ¹H-NMR, indicating more strongly thermally populated triplet states for longer molecules.

We optimized the molecular structures in the closed-shell, open-shell singlet (bs), and triplet states with the four xc functionals under consideration. Here, we employed Grimme’s empirical dispersion correction (D3)⁸², since it has been proven important for extended organic systems. We had not employed this correction for the inorganic complexes above, because its suitability for inorganic systems is not as clearly established as for organic ones⁷⁶.

For all functionals and structures, we obtain either a closed-shell solution as the ground state, or an open-shell singlet (bs) that is close in energy to the closed-shell one. The energy differences between the two are at most around 3.5 kJ/mol, which appears too close to the DFT error margin to make a well-founded decision on which of the two represents the ground state better. The \hat{S}^2 expectation values of the bs solutions are often close to zero and never larger than about 0.6, indicating partial closed-shell character (see Table S5 in the Supporting Information). The larger $\langle \hat{S}^2 \rangle$, the more the structural diradical characters y_s and bond-length alternation deviate from the “true” closed-shell solution. In all cases, the triplets are considerably higher in energy, consistent with the dominantly closed-shell ground states, and the singlet–triplet splitting of 27 kJ/mol obtained from B3LYP-D3 is consistent with the 22 kJ/mol obtained from temperature-dependent magnetic susceptibility measurements of the **bab** powder and with the 23 kJ/mol obtained previously from UCAM-B3LYP/6-31G(d,p)⁴³. This is also in line with the singlet y_s always being considerably lower than the triplet values, suggesting that no singlet has bond length patterns corresponding to pure open-shell structures.

The structural diradical characters y_s for the B3LYP-D3 closed-shell solutions match the

experiment almost perfectly. For the longest molecule **bab**, the bs optimization converges to structures with a $\langle \hat{S}^2 \rangle$ value of roughly 0.6, which is slightly lower in energy and features a larger y_s than the cs solution (0.71 vs. 0.63). Given the quite small energy differences, this bs solution may be an artifact of DFT. It could also be that the good match of the cs data results from an error compensation between the electronic structure description and the neglect of crystal packing effects (compare the discussion in the preceding section). Without the experimental data, there would be little solid criteria for deciding which of the two describes the experiment better. As exact exchange admixtures increase in the functionals, the structural diradical characters of the closed-shell solutions increase slightly, leading to an overestimation of the experimental values (that could still be consistent with the experiment if packing effects should play a role).

MAE values between optimized and experimental geometries showed a very good correlation with y_{el} values ranging from 1.00 for **bbb** to 0.98 for **bab**. The correlation between y_s and y_{el} is slightly smaller ranging from 0.99 for **bbb** to 0.88 for **bab**. This means that for organic systems, both y_s and MAE are well suited.

Bond length alternation decreases as the molecules get longer, which is consistent with the increasing diradical character. Also if BLA is taken as a criterion, closed-shell B3LYP-D3 matches the experiment well, slightly overestimating BLA, while TPSSh errs in the other direction showing the best agreement of the functionals considered. For these organic systems, BLA is much more consistent over different functionals, and the conclusions drawn from BLA and y_s are similar: the two hybrid functionals are suited best to describe bond length patterns in these organic diradical candidates. This good agreement between the two measures may be because (1) BLA is more suitable for organic systems than for inorganic ones, and because (2) the same sets of bonds are employed in evaluating these measures here, in contrast to the diiron and dicobalt complexes discussed above. Furthermore, while experimental error bars on bond lengths still affect BLA values more than y_s , this is much less severe than it was the case for the two diiron complexes discussed above, so for organic systems, both BLA and y_s appear as reasonable choices for evaluating agreement between calculated and experimental bond length patterns.

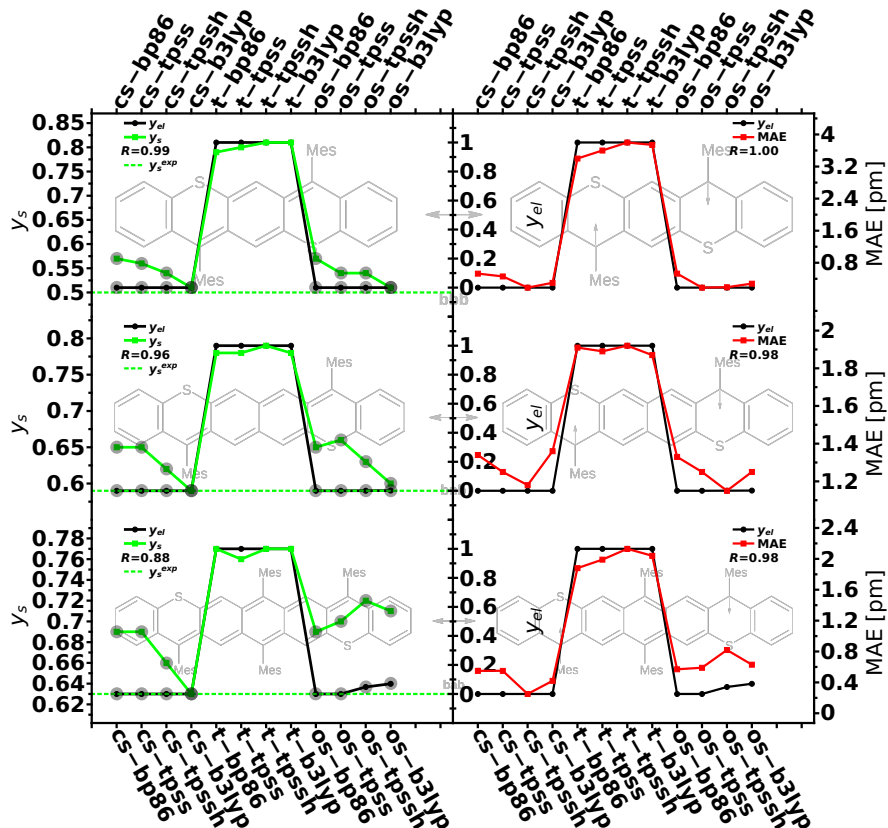


FIG. 8. Comparison of the correlation between electronic diradical character y_{el} and structural diradical character y_s (MAE) on the left (right). MAE values are calculated from geometry optimized- and experimental structures. The Pearson correlation coefficient R is shown in the corresponding legends. The data for **bbb** are shown in the top third, for **bnb** are shown in the center third and for **bab** are shown in the bottom third. Values for y_{el} , y_s and MAE are plotted against a string representing the calculated determinant (either cs for closed shell, t for triplet or os for broken symmetry) and the used xc functional. Additionally, the calculated structural diradical character values for the x-ray structures y_s^{exp} are plotted as a constant dotted line. The energetically most stable structures are highlighted by a circular grid on top of the data point. Again, energies differing by less than 5 kJ are considered degenerate, leading to multiple highlighted structures per functional in some cases.

VI. CONCLUSION

For predicting nonlinear optical properties of molecules, it is essential to provide correct molecular structures based on first-principles electronic structure methods. For this purpose,

small absolute errors are not sufficient, but also a reliable description of relative structural parameters such as bond length patterns is necessary. We have therefore suggested a new measure, structural diradical character y_s , which is based on comparisons between molecular structures and idealized closed-shell and diradical structures. We can show that with this new measure, consistent comparisons between experiment and first-principles molecular structures for diradicals are possible.

Based on these comparisons, we can identify two hybrid functionals, TPSSh and B3LYP, with 10 and 20 percent of exact exchange admixture, as suitable for describing structural diradical character in both organic and organometallic systems. B3LYP (with Grimme’s empirical dispersion corrections) works best for the organic molecules, and TPSSh (without dispersion correction) for the organometallic complexes under study. Importantly, these functionals were also the ones which gave a realistic description of singlet–triplet energy differences. The GGA and meta-GGA functionals BP86 and TPSS turned out not suitable for neither purpose.

The excellent agreement for B3LYP-D3 was only found when the organic molecules (a series of bisbenzothiaquinodimethanes with different molecular lengths) were described as closed-shell electronic structures (restricted KS-DFT), even though in some cases broken-symmetry solutions with partial open-shell singlet character were slightly lower in energy, but within typical DFT error bars (up to 3.5 kJ/mol). This illustrates that present-day KS DFT may be unable to make predictions in cases like these, where closed-shell and open-shell singlets are close in energy. On the upside, there exists one frequently used functional, B3LYP, which is able to provide perfect agreement for these structures when only the closed-shell singlets are considered. Possibly, these data could indicate that when singlet–triplet gaps are large, and when closed- and open-shell singlets are nearly degenerate, one should consider the closed-shell singlets as more reliable for present-day standard xc functionals. However, such statements clearly require more research, possibly also considering schemes which combine a more explicit description of static correlation with Kohn–Sham DFT^{83–87}.

Comparing structural diradical character y_s obtained from experiment with assignments as (predominantly) open-shell or closed-shell from the literature suggests that y_s smaller than roughly 0.6 (with MAE as a measure for structural deviations) points to a more closed-shell structure, while larger y_s correspond to more open-shell structures. Closeness to triplet y_s values may also serve as an absolute criterion for pure open-shell character (usually

only applicable to computed structures, however). For closed-shell electronic structures, y_s slightly decreases with increasing exact exchange admixture, while for open-shell singlet, it increases, so that differences between the two structures become more pronounced.

Our work was motivated by our attempt at a true first-principles prediction of the open-shell character for a photoswitchable [Co₂] complex, which may be a structure worth pursuing and optimizing further for achieving photoswitchable NLO properties. Our findings imply that B3LYP, which suggests an open-shell singlet ground state, is more reliable than BP86, which favors the closed-shell singlet. Therefore, further research into this and related compounds, and their switchability, appears a worthwhile avenue of research.

It is challenging to define diradical measures which are also applicable to experimental data (with a notable exception suggested by Kamada et al.⁸⁸). Therefore, beyond such comparisons between theory and experiment, structural diradical character may also be interesting as a complement to electronic diradical character. This will require generalizing the definition of reference structural parameters, e.g. for structures where diradical character correlates with the presence or absence of a tin–tin bond rather than bond length alternation.

VII. ACKNOWLEDGMENT

The authors acknowledge funding by the German Research Foundation (DFG) via SFB 668, the high-performance-computing team of the Regional Computer Center at University of Hamburg and the North-German Supercomputing Alliance (HLRN) for technical support and computational resources. The authors thank Markus Reiher, ETH Zurich, and Jürgen Heck, University of Hamburg, for valuable discussions.

Appendix A: Critical discussion of bond length alternation (BLA) as a measure for comparing diradical structures

BLA^{39,40} is evaluated as the average difference between bond lengths for N pairs of adjacent bonds ($b_{i,0}$ and $b_{i,1}$),

$$\text{BLA} = \frac{1}{N} \sum_{i=1}^N b_{i,0} - b_{i,1}, \quad (\text{A1})$$

which, e.g., can be alternating single and double or alternating single and triple bonds.^{39,40} The bonds that were considered for the BLA are shown in the corresponding figures in red if they were added and in blue if they were subtracted.

Using BLA as a measure for diradical character has some drawbacks. (i) The BLA can only be used for one sort of alternating bonds, while for the iron complexes ($[\text{Fe}_2]$ and $[\text{Fe}_2]'$) there are both alternating single and double bonds, as well as alternating single and triple bonds. One has to choose which set of bonds will be used for calculating the BLA and which will be dismissed. Also, for some inorganic structures such as the tin cluster studied in Ref.⁸⁹, diradical character correlates with the presence or absence of a tin–tin bond rather than bond length alternation. (ii) Pairs of bonds have to be used, meaning that an even number of bonds must be considered. For example, for the biscobaltocenyldithienylethene ($[\text{Co}_2]$) this is not the case, and one has to choose arbitrarily one bond which will not be taken into account. (iii) The sign of the calculated BLA is choice-dependent and could be switched by adding the bond lengths that were subtracted and vice versa. This indicates that it is difficult to define a unique and transferable measure for diradical character based on bond-length alternation. (iv) The calculated numbers for different systems cannot be directly compared, because the magnitude of the numbers is system-dependent. (v) BLA measures bond length patterns in absolute terms, which implies that when comparing calculated with experimental data, deviations resulting from a general over- or underestimation of bond lengths by a given functional are mixed with those resulting from an inadequate representation of relative bond lengths differences.

Appendix B: Theoretical methods

All electronic structure calculations were performed using the TURBOMOLE 6.5 program package imposing no symmetry (C_1 symmetry) on the systems. A value of 10^{-7} a.u. was set as the convergence criterion for the energy during self-consistent field calculations. For the molecular structure optimizations the threshold was set to 10^{-6} a.u. for the energy change, to 10^{-3} a.u. for the maximum displacement element, to 10^{-4} a.u. for the maximum gradient element, to $5 \cdot 10^{-4}$ a.u. for the root mean square of the displacement, and to $5 \cdot 10^{-4}$ a.u. for the root mean square of the gradient. The employed xc functional (either BP86^{90,91}, TPSS⁹², TPSSH^{93,94} or B3LYP^{95–97}) and basis set (either def-TZVP^{98,99} or def2-

TZVP^{100,101}) and whether the third generation empirical dispersion correction of Grimme (D3)¹⁰² was used or not is indicated in the respective tables.

For the closed-shell calculations restricted KS-DFT was employed. In order to obtain the broken-symmetry determinants, an unrestricted KS-DFT calculation of the triplet state was performed and followed by a subsequent broken-symmetry calculation using Turbomole’s “flip” option on the triplet determinant for obtaining the initial guess for the broken-symmetry calculation. The calculated ground state was then determined by comparison of the energies of the determinants and their corresponding $\langle \hat{S}^2 \rangle$ values.

Appendix C: On the applicability of broken-symmetry density functional theory for structural optimizations of diradicals

A closed-shell determinant will always have a $\langle \hat{S}^2 \rangle$ value of zero, while an open-shell determinant representing a diradicaloid will have a $\langle \hat{S}^2 \rangle$ value larger than zero. This is referred to as spin contamination. For discussions on the validity of broken-symmetry energies, see, e.g., Refs.^{103–111}. On the one hand, it is argued that the Kohn–Sham reference system of noninteracting fermions should have the same $\langle \hat{S}^2 \rangle$ value as the real, interacting system, and following this argument, schemes have been suggested for estimating the molecular structure of the spin-projected open-shell singlet based on broken-symmetry calculations¹¹². On the other hand, it is not generally established how to evaluate the $\langle \hat{S}^2 \rangle$ value of the interacting system in Kohn–Sham DFT, and there is no unique established way for handling possible double counting of electron correlation when employing spin projection on top of broken-symmetry Kohn–Sham determinants^{83–86}. In practice, the Broken-Symmetry approach has been very successful in modeling molecular structures and energetics of antiferromagnetically coupled systems^{79,103}. We therefore take a pragmatic approach here, directly evaluating the broken-symmetry energies as those of the open-shell singlet. For future work, it would be interesting to consider schemes which combine a more explicit description of static correlation with Kohn–Sham DFT^{83–87}. At present, these are too computationally expensive for routine structural optimizations of molecules of the size under study here.

REFERENCES

- ¹Abe, M. *Chem Rev* 2013, 113, 7011.
- ²Enoki, T.; Ando, T. *Physics and chemistry of graphene: graphene to nanographene*; CRC Press, 2013.
- ³Lambert, C. *Angew Chem Int Ed* 2011, 50, 1756.
- ⁴Sun, Z.; Ye, Q.; Chi, C.; Wu, J. *Chem Soc Rev* 2012, 41, 7857.
- ⁵Jung, Y.; Head-Gordon, M. *J Phys Chem A* 2003, 107, 7475.
- ⁶Michl, J. *J Am Chem Soc* 1996, 118, 3568.
- ⁷Salem, L.; Rowland, C. *Angew Chem, Int Ed* 1972, 11, 92.
- ⁸Lineberger, W. C.; Borden, W. T. *Phys Chem Chem Phys* 2011, 13, 11792.
- ⁹Lenhardt, J. M.; Ong, M. T.; Choe, R.; Evenhuis, C. R.; Martinez, T. J.; Craig, S. L. *Science* 2010, 329, 1057.
- ¹⁰Stuyver, T.; Fias, S.; Proft, F. D.; Geerlings, P.; Tsuji, Y.; Hoffmann, R. *J Chem Phys* 2017, 146, 092310.
- ¹¹Nakano, M.; Champagne, B. *J Chem Phys* 2013, 138, 244306.
- ¹²Nanda, K. D.; Krylov, A. I. *J Chem Phys* 2017, 146, 224103.
- ¹³Bonness, S.; Botek, E.; Champagne, B. *J Chem Phys* 2010, 132, 094107.
- ¹⁴Inoue, Y.; Yamada, T.; Champagne, B.; Nakano, M. *Chem Phys Lett* 2013, 570, 75.
- ¹⁵Yamada, T.; Takamuku, S.; Matsui, H.; Champagne, B.; Nakano, M. *Chem Phys Lett* 2014, 608, 68.
- ¹⁶Hatua, K.; Nandi, P. K. *Chem Phys Lett* 2015, 628, 1.
- ¹⁷Nakano, M.; Champagne, B. *Wiley Interdiscip Rev Comput Mol Sci* 2016, 6, 198.
- ¹⁸Muhammad, S.; Nakano, M.; Al-Sehemi, A. G.; Kitagawa, Y.; Irfan, A.; Chaudhry, A. R.; Kishi, R.; Ito, S.; Yoneda, K.; Fukuda, K. *Nanoscale* 2016, 8, 17998.
- ¹⁹Castet, F.; Rodriguez, V.; Pozzo, J.-L.; Ducasse, L.; Plaquet, A.; Champagne, B. *Acc Chem Res* 2013, 46, 2656.
- ²⁰Beaujean, P.; Bondu, F.; Plaquet, A.; Garcia-Amorós, J.; Cusido, J.; Raymo, F. M.; Castet, F.; Rodriguez, V.; Champagne, B. *J Am Chem Soc* 2016, 138, 5052.
- ²¹Sun, Z.; Chen, T.; Liu, X.; Hong, M.; Luo, J. *J Am Chem Soc* 2015, 137, 15660.
- ²²Attar, S.; Espa, D.; Artizzu, F.; Pilia, L.; Serpe, A.; Pizzotti, M.; Carlo, G. D.; Marchio, L.; Deplano, P. *Inorg Chem* 2017, 56, 6763.

- ²³Cariati, E.; Liu, X.; Geng, Y.; Forni, A.; Lucenti, E.; Righetto, S.; Decurtins, S.; Liu, S.-X. *Phys Chem Chem Phys* 2017, 19, 22573.
- ²⁴Schulze, M.; Utecht, M.; Moldt, T.; Przyrembel, D.; Gahl, C.; Weinelt, M.; Saalfrank, P.; Tegeder, P. *Phys Chem Chem Phys* 2015, 17, 18079.
- ²⁵Okuno, K.; Shigeta, Y.; Kishi, R.; Nakano, M. *J Phys Chem Lett* 2013, 4, 2418.
- ²⁶Torrent-Sucarrat, M.; Navarro, S.; Marcos, E.; Anglada, J. M.; Luis, J. M. *J Phys Chem C* 2017, 121, 19348.
- ²⁷Florindo, P. R.; Costa, P. J.; Piedade, M. F. M.; Robalo, M. P. *Inorg Chem* 2017, 56, 6849.
- ²⁸Nakano, M.; Kishi, R.; Nitta, T.; Kubo, T.; Nakasuji, K.; Kamada, K.; Ohta, K.; Champagne, B.; Botek, E.; Yamaguchi, K. *J Phys Chem A* 2005, 109, 885.
- ²⁹Vila, F. D.; Strubbe, D. A.; Takimoto, Y.; Andrade, X.; Rubio, A.; Louie, S. G.; Rehr, J. J. *J Chem Phys* 2010, 133, 034111.
- ³⁰Seidler, T.; Stadnicka, K.; Champagne, B. *J Chem Theory Comput* 2014, 10, 2114.
- ³¹Sherrill, C. D.; Seidl, E. T.; Schaefer III, H. F. *J Phys Chem* 1992, 96, 37123716.
- ³²Bahlke, M. P.; Karolak, M.; Herrmann, C. *Phys Rev B* 2018, 97, 035119.
- ³³Skornyakov, S. L.; Anisimov, V. I.; Vollhardt, D.; Leonov, I. *Phys Rev B* 2017, 96, 035137.
- ³⁴Plihal, M.; Langreth, D. C. *Phys Rev B* 1998, 58, 2191.
- ³⁵Matsuda, K.; Irie, M. *Tetrahedron Lett* 2000, 41, 2577.
- ³⁶Kawai, S. H.; Gilat, S. L.; Lehn, J.-M. *Chem Commun* 1994, , 1011.
- ³⁷Escribano, A.; Steenbock, T.; Stork, C.; Herrmann, C.; Heck, J. *ChemPhysChem* 2017, 18, 596.
- ³⁸Matsuda, K.; Irie, M. *J Am Chem Soc* 2000, 122, 7195.
- ³⁹Chalifoux, W. A.; McDonald, R.; Ferguson, M. J.; Tykwinski, R. R. *Angew Chem Int Ed* 2009, 48, 7915.
- ⁴⁰Bylaska, E. J.; Weare, J. H.; Kawai, R. *Phys Rev B* 1998, 58, R7488.
- ⁴¹de Montigny, F.; Argouarch, G.; Costuas, K.; Halet, J.-F.; Roisnel, T.; Toupet, L.; Lapinte, C. *Organometallics* 2005, 24, 4558.
- ⁴²Paul, F.; Bondon, A.; da Costa, G.; Malvolti, F.; Sinbandhit, S.; Cador, O.; Costuas, K.; Toupet, L.; Boillot, M.-L. *Inorg Chem* 2009, 48, 10608.
- ⁴³Dong, S.; Heng, T. S.; Gopalakrishna, T. Y.; Phan, H.; Lim, Z. L.; Hu, P.; Webster, R. D.; Ding, J.; Chi, C. *Angew Chem* 2016, 128, 9462.

- ⁴⁴Haynes, W. M. CRC Handbook of Chemistry and Physics, 97th Edition -; CRC Press: Boca Raton, Fla, 2016.
- ⁴⁵For structures such as the tin cluster referred to above⁸⁹, one could define reference bond lengths for typical tin–tin single bonds for the closed-shell and the sum of two tin van-der-Waals radii for the open-shell structure. This structure would clearly be a challenge for structural measures of diradical character.
- ⁴⁶Craig, N. C.; Groner, P.; McKean, D. C. J Phys Chem A 2006, 110, 7461.
- ⁴⁷Nakano, M.; Fukuda, K.; Ito, S.; Matsui, H.; Nagami, T.; Takamuku, S.; Kitagawa, Y.; Champagne, B. J Phys Chem A 2017, 121, 861.
- ⁴⁸Ramos-Cordoba, E.; Salvador, P. Phys Chem Chem Phys 2014, 16, 9565.
- ⁴⁹Bachler, V.; Olbrich, G.; Neese, F.; Wieghardt, K. Inorg Chem 2002, 41, 4179.
- ⁵⁰Herebian, D.; Wieghardt, K. E.; Neese, F. J Am Chem Soc 2003, 125, 10997.
- ⁵¹Braida, B.; Galembeck, S. E.; Hiberty, P. C. J Chem Theory Comput 2017, 13, 3228.
- ⁵²Neese, F. J Phys Chem Sol 2004, 65, 781.
- ⁵³Noodleman, L. J Chem Phys 1981, 74, 5737.
- ⁵⁴“Spin center” refers to the metal atoms in the organometallic complexes, and to the formally spin-bearing carbon atoms in the diradical resonance structure for the organic structures.
- ⁵⁵Szabo, A.; Ostlund, N. S. Modern Quantum Chemistry: Introduction to Advanced Electronic Structure Theory; Dover Publications: New York, 1996.
- ⁵⁶Shil, S.; Herrmann, C. J Comput Chem 2018. Accepted, DOI 10.1002/jcc.25153.
- ⁵⁷Nenon, S.; Champagne, B. J Chem Phys 2013, 138, 204107.
- ⁵⁸Seidler, T.; Stadnicka, K.; Champagne, B. J Chem Phys 2013, 139, 114105.
- ⁵⁹Champagne, B.; Perpete, E. A.; Jacquemin, D.; van Gisbergen, S. J. A.; Baerends, E.-J.; Soubra-Ghaoui, C.; Robins, K. A.; Kirtman, B. J Phys Chem A 2000, 104, 4755.
- ⁶⁰Bulat, F. A.; Toro-Labbe, A.; Champagne, B.; Kirtman, B.; Yang, W. J Chem Phys 2005, 123, 014319.
- ⁶¹Sekino, H.; Maeda, Y.; Kamiya, M.; Hirao, K. J Chem Phys 2007, 126, 014107.
- ⁶²Jacquemin, D.; Perpete, E. A.; Medved, M.; Scalmani, G.; Frisch, M. J.; Kobayashi, R.; Adamo, C. J Chem Phys 2007, 126, 191108.
- ⁶³Suponitsky, K. Y.; Tafur, S.; Masunov, A. E. J Chem Phys 2008, 129, 044109.
- ⁶⁴Borini, S.; Limacher, A., P.; Luthi, H. P. J Chem Phys 2009, 131, 124105.

- ⁶⁵Karamanis, P.; Marchal, R.; Carbonniere, P.; Pouchan, C. *J Chem Phys* 2011, 135, 044511.
- ⁶⁶Sun, H.; Autschbach, J. *ChemPhysChem* 2013, 14, 2450.
- ⁶⁷Garrett, K.; Vazquez, X. S.; Egri, S. B.; Wilmer, J.; Johnson, L. E.; Robinson, B. H.; Isborn, C. M. *J Chem Theory Comput* 2014, 10, 3821.
- ⁶⁸Garza, A. J.; Osman, O. I.; Asiri, A. M.; Scuseria, G. E. *J Phys Chem B* 2015, 119, 1202.
- ⁶⁹Wang, C.; Yuan, Y.; Tian, X. *J Comput Chem* 2017, 38, 594.
- ⁷⁰Kishi, R.; Bonness, S.; Yoneda, K.; Takahashi, H.; Nakano, M.; Botek, E.; Kubo, B. C. T.; Kamada, K.; Ohta, K.; Tsuneda, T. *J Chem Phys* 2010, 132, 094107.
- ⁷¹Büchert, M.; Steenbock, T.; Lukaschek, C.; Wolff, M. C.; Herrmann, C.; Heck, J. *Chem Eur J* 2014, 20, 14351.
- ⁷²Ye, A.; Patchkovskii, S.; Autschbach, J. *J Chem Phys* 2007, 127, 074104.
- ⁷³Ye, A.; Autschbach, J. *J Chem Phys* 2006, 125, 234101.
- ⁷⁴Furche, F.; Perdew, J. P. *J Chem Phys* 2006, 124, 044103.
- ⁷⁵Waller, M. P.; Braun, H.; Hojdis, N.; Bühl, M. *J Chem Theory Comput* 2007, 3, 2234.
- ⁷⁶Weymuth, T.; Couzijn, E. P. A.; Chen, P.; Reiher, M. *J Chem Theory Comput* 2014, 10, 3092.
- ⁷⁷Herrmann, C.; Reiher, M.; Hess, B. A. *J Chem Phys* 2005, 122, 034102.
- ⁷⁸Herrmann, C.; Yu, L.; Reiher, M. *J Comput Chem* 2006, 27, 1223.
- ⁷⁹Cramer, C. J.; Truhlar, D. G. *Phys Chem Chem Phys* 2009, 11, 10757.
- ⁸⁰Interpolated data between the two structures can be found in the Supporting Information.
- ⁸¹Trinquier, G.; Malrieu, J.-P. *Chem Eur J* 2016, 21, 814.
- ⁸²Grimme, S. *Wiley Interdiscip Rev Comput Mol Sci* 2011, 1, 211.
- ⁸³Li Manni, G.; Carlson, R. K.; Luo, S.; Ma, D.; Olsen, J.; Truhlar, D. G.; Gagliardi, L. *J Chem Theory Comput* 2014, 10, 3669.
- ⁸⁴Hubert, M.; Hedegard, E. D.; Jensen, H. J. A. *J Chem Theory Comput* 2016, 12, 2203.
- ⁸⁵Knecht, E. D. H. S.; Kielberg, J. S.; Jensen, H. J. A.; Reiher, M. *J Chem Phys* 2015, 142, 224108.
- ⁸⁶Garza, A. J.; Jiménez-Hoyos, C. A.; Scuseria, G. E. *J Chem Phys*, 2014, 140, 244102.
- ⁸⁷Stoneburner, S. J.; Truhlar, D. G.; Gagliardi, L. *J Chem Phys* 2018, 148, 064108.
- ⁸⁸Kamada, K.; Ohta, K.; Shimizu, A.; Kubo, T.; Kishi, R.; Takahashi, H.; Botek, E.; Champagne, B.; Nakano, M. *J Phys Chem Lett* 2010, 1, 937.

- ⁸⁹Schrenk, C.; Kubas, A.; Fink, K.; Schnepf, A. *Angew Chem Int Ed* 2011, 50, 7273.
- ⁹⁰Becke, A. D. *Phys Rev A* 1988, 38, 3098.
- ⁹¹Perdew, J. P. *Phys Rev B* 1986, 33, 8822.
- ⁹²Tao, J.; Perdew, J. P.; Staroverov, V. N.; Scuseria, G. E. *Phys Rev Lett* 2003, 91, 146401.
- ⁹³Tao, J.; Perdew, J. P.; Staroverov, V. N.; Scuseria, G. E. *Phys Rev Lett* 2003, 91, 146401.
- ⁹⁴Staroverov, V. N.; Scuseria, G. E.; Tao, J.; Perdew, J. P. *J Chem Phys* 2003, 119, 12129.
- ⁹⁵Becke, A. D. *J Chem Phys* 1993, 98, 5648.
- ⁹⁶Lee, C.; Yang, W.; Parr, R. G. *Phys Rev B* 1988, 37, 785.
- ⁹⁷Miehlich, B.; Savin, A.; Stoll, H.; Preuss, H. *Chem Phys Lett* 1989, 157, 200.
- ⁹⁸Schäfer, A.; Horn, H.; Ahlrichs, R. *J Chem Phys* 1992, 97, 2571.
- ⁹⁹Schäfer, A.; Huber, C.; Ahlrichs, R. *J Chem Phys* 1994, 100, 5829.
- ¹⁰⁰Weigend, F.; Ahlrichs, R. *Phys Chem Chem Phys* 2005, 7, 3297.
- ¹⁰¹Weigend, F. *Phys Chem Chem Phys* 2006, 8, 1057.
- ¹⁰²Grimme, S.; Antony, J.; Ehrlich, S.; Krieg, H. *J Chem Phys* 2010, 132, 154104.
- ¹⁰³Ruiz, E.; Cano, J.; Alvarez, S.; Alemany, P. *J Comput Chem* 1999, 20, 1391.
- ¹⁰⁴de P. R. Moreira, I.; Illas, F. *Phys Chem Chem Phys* 2006, 8, 1645.
- ¹⁰⁵Perdew, J.; Savin, A.; Burke, K. *Phys Rev A* 1995, 51, 4531.
- ¹⁰⁶Jacob, C.; Reiher, M. *Int J Quantum Chem* 2012, 112, 3661.
- ¹⁰⁷Cohen, A. J.; Tozer, D. J.; Handy, N. C. *J Chem Phys* 2007, 126, 214104.
- ¹⁰⁸Wang, J.; Becke, A. D.; Smith, Jr., V. H. *J Chem Phys* 1995, 102, 3477.
- ¹⁰⁹Bauer, G. E. W. *Phys Rev B* 1983, 27, 5912.
- ¹¹⁰Görling, A.; Levy, M.; Perdew, J. P. *Phys Rev B* 1993, 47, 1167.
- ¹¹¹Davidson, E. R.; Clark, A. E. *Int J Quantum Chem* 2005, 103, 1.
- ¹¹²Malrieu, J.-P.; Trinquier, G. *J Phys Chem A* 2012, 116, 8226.